the σ electrons dominate and generate delocalized structures. The enforced delocalization of π electrons is the origin of the aromatic properties of such ring systems. In five-membered heterocycles with six π electrons, the general trends are similar, but no dominance of either σ or π part can be found. The equilibrium structure is a compromise between localized and delocalized structures, but some delocalization remains. The aromaticity is consequently less pronounced. Nonaromatic and antiaromatic rings prefer localized structures, where the antiaromatic compounds are more localized than the nonaromatic compounds. This is expressed in a minimum of the π curve and a maximum of the σ curve at equilibrium. Finally, the removal of π electrons can cause the π curve to revert its trend from a preference for a localized to a preference for a delocalized structure. The properties attributed to aromaticity definitely depend on the π electrons and their delocalization, but the origin of delocalized structures in neutral ring compounds is due to the σ electrons.

Acknowledgment. The calculations were performed on a CYBER 180-990 at RRZN Hannover.

Projection Operator Hückel Method and Antiferromagnetism

Stephen Lee

Contribution from the Department of Chemistry, University of Michigan, Ann Arbor, Michigan 48109-1055. *Received January 16, 1990*

Abstract: We present a simple molecular orbital method by which the antiferromagnetism of $KCuF_3$, La_2CuO_4, and other one electron per atom or one hole per atom systems can be understood. The roles of alternacy and nonalternacy and of spatial distortions in producing the observed antiferromagnetic ordering are shown to be important. This simple molecular orbital method is also shown to be reliable in understanding the energetics of a model spin-Peierls system.

The extended Hückel (eH) method[1] has been shown to be successful in rationalizing many structural features found in solid-state chemistry. Questions of unusual coordination environments, metal–metal bonding, patterns of bond breaking or bond formation, and site preferences in materials that range from intermetallic alloys to halides have been studied by eH methods. There are several good review articles that summarize these results.[2]

In this paper we show that a technique which incorporates Hückel or eH calculations can be used in understanding strong antiferromagnetic spin–spin correlations. This approach is based on the work of many groups who have found a remarkable coincidence between molecular orbitals models and the spin Hamiltonians generally used in studies of ferromagnetic and antiferromagnetic systems.[3] The methods that have been used vary from Lie group and quasi-spin approaches, Rumer diagram techniques,[4] Pariser–Parr–Pople or Hubbard models and quantum Monte Carlo simulations,[5] effective Heisenberg Hamiltonians,[6] and the Gutzwiller approximation.[7] Although these models are technically involved, the results we will use in this work are quite simple. Indeed, one of the goals of this article is to recast the findings of these various workers in a form that can readily be used by chemists who are familiar with molecular orbital (MO) theory but who have never performed, for example, a quantum Monte Carlo simulation. We illustrate the utility of our technique by studying the antiferromagnetic (AF) ordering of $KCuF_3$[8] and La_2CuO_4[9] and the spin-Peierls distortion.[10]

(1) (a) Hoffmann, R. *J. Chem. Phys.* **1963**, *39*, 1397. (b) Hoffmann, R.; Lipscomb, W. N. *Ibid.* **1962**, *36*, 2179. (c) Whangbo, M.-H.; Hoffmann, R.; Woodward, R. B. *Proc. R. Soc.* **1979**, *A366*, 23.

(2) (a) Hoffmann, R. *Solids and Surfaces: A Chemist's View of Bonding in Extended Structures*; VCH Publishers: New York, 1988. (b) Burdett, J. K. *Prog. Solid State Chem.* **1984**, *15*, 173. (c) Whangbo, M.-H. In *Crystal Chemistry and Properties of Materials with Quasi-One Dimensional Structure*; Rouxel, J., Ed.; Reidel: Dordrecht, 1986; p 27.

(3) (a) Lieb, E.; Schultz, T.; Mattis, D. *Ann. Phys.* **1961**, *16*, 407. (b) Lieb, E.; Mattis, D. *J. Math. Phys.* **1962**, *3*, 749. (c) Mattis, D. *The Theory of Magnetism I*; Springer-Verlag: Berlin, 1981. (d) Anderson, P. W. *Magnetism*; Rado, G. T., Suhl, H., Eds.; Academic: New York, 1966; Vol. 1.

(4) (a) Klein, D. J.; Nelin, C. G.; Alexander, S. A.; Matsen, F. A. *J. Chem. Phys.* **1982**, *77*, 3101. (b) Klein, D. J. *J. Chem. Phys.* **1982**, *77*, 3098. (c) Shiba, H.; Pincus, P. *Phys. Rev. B* **1972**, *5*, 1966. (d) Herrick, D. R.; Liao, C.-L. *J. Chem. Phys.* **1981**, *75*, 4485. (e) Herrick, D. R. *Adv. Chem. Phys.* **1983**, *52*, 1. (f) Matsen, F. A.; Welsher, T. L. *Int. J. Quantum Chem.* **1977**, *12*, 985, 1001. (g) Cizek, J.; Pauncz, R.; Vrscay, E. R. *J. Chem. Phys.* **1983**, *78*, 3807. (h) Bondeson, S. R.; Soos, Z. G. *J. Chem. Phys.* **1979**, *71*, 3807. (i) Klein, D. J.; Trinajstic, N. *J. Am. Chem. Soc.* **1984**, *106*, 8050. (j) Alexander, S. A.; Klein, D. J. *J. Am. Chem. Soc.* **1988**, *110*, 3401.

(5) (a) Hirsch, J. E.; Scalapino, D. J.; Sugar, R. L. *Phys. Rev. Lett.* **1981**, *47*, 1628. (b) Hirsch, J. E. *Phys. Rev. Lett.* **1983**, *51*, 1900. (c) Hirsch, J. E.; Sugar, R. L.; Scalapino, D. J.; Blankenbecker, R. *Phys. Rev. B* **1982**, *26*, 5033. (d) Scalapino, D. J.; Loh, E., Jr.; Hirsch, J. E. *Phys. Rev. B* **1986**, *34*, 8190. (e) Lin, H. Q.; Hirsch, J. E. *Phys. Rev. B* **1986**, *34*, 1964. (f) Hirsch, J. E. *Phys. Rev. B* **1985**, *31*, 403. (g) Hirsch, J. E. *Phys. Rev. B* **1986**, *34*, 3216. (h) Hubbard, J. *Proc. Roy. Soc. London A* **1963**, *276*, 283.

(6) (a) Said, M.; Maynau, D.; Malrieu, J.-P. *J. Am. Chem. Soc.* **1984**, *106*, 580. (b) Said, M.; Maynau, D.; Malrieu, J.-P.; Garcia-Bach, M.-A. *J. Am. Chem. Soc.* **1984**, *106*, 571. (c) Durand, P.; Malrieu, J.-P. In *Ab Initio Methods in Quantum Chemistry*; Lawley, K. P., Ed.; J. Wiley: New York, 1987. (d) Maynau, D.; Durand, P.; Daudey, J. P.; Malrieu, J.-P. *Phys. Rev. A* 1983, *28*, 3193. (e) Pellegatti, A.; Marinelli, F.; Roche, M.; Maynau, D.; Malrieu, J.-P. *J. Phys. C. Solid State Phys.* **1987**, *20*, 5141. (f) de Loth, P.; Malrieu, J.-P. *J. Physique* **1987**, *48*, 29. (g) Hiberty, P. C.; Ohanessian, G. *Int. J. Quantum Chem.* **1985**, *27*, 259. (h) Ouija, B.; Lepetit, M.-B.; Maynau, D.; Malrieu, J.-P. *Phys. Rev. A* **1989**, *39*, 3274, 3289. (i) Maynau, D.; Garcia-Bach, M. A.; Malrieu, J.-P. *J. Physique* **1986**, *47*, 207. (j) Maynau, D.; Malrieu, J.-P. *J. Chem. Phys.* **1988**, *88*, 3163. (k) Lee, S. *J. Chem. Phys.* **1989**, *90*, 2732, 2741. (l) Lee, S. *J. Am. Chem. Soc.* **1989**, *111*, 7754. (m) Gautier, F. In *Magnetism of Metals and Alloys*; Cyrot, M., Ed.; North Holland: Amsterdam, 1982.

(7) (a) Kaplan, T. A.; Horsch, P.; Fulde, P. *Phys. Rev. Lett.* **1982**, *49*, 889. (b) Horsch, P.; Kaplan, T. A. *J. Phys. C: Solid State Phys.* **1983**, *16*, L1203. (c) Horsch, P.; Kaplan, T. A. *Bull. Am. Phys. Soc.* **1985**, *30*, 513. (d) Gutzwiller, M. C. *Phys. Rev.* **1965**, *137*, A1726.

(8) (a) Okazaki, A.; Suemune, Y. *J. Phys. Soc. Jpn.* **1961**, *16*, 176. (b) Okazaki, A. *J. Phys. Soc. Jpn.* **1969**, *26*, 870.

(9) (a) Longo, J. M.; Raccah, P. M. *J. Solid State Phys.* **1983**, *16*, L1203. (b) Müller-Buschbaum, H.; Lehmann, U. *Z. Anorg. Allg. Chem.* **1978**, *447*, 47. (c) Grande, B.; Müller-Buschbaum, H.; Schweizer, M. *Z. Anorg. Allg. Chem.* **1977**, *428*, 120. (d) Chaillout, C.; Cheong, S. W.; Fisk, Z.; Lehmann, M. S.; Marezio, M.; Morosin, B.; Schirber, J. E. *Physica C* **1989**, *158*, 183.

0002-7863/90/1512-6777$02.50/0

The Projection Operator Hückel Method

The method is simply illustrated by considering the π atomic orbitals of **1**, butadiene, where the individual orbitals are labeled a through d.

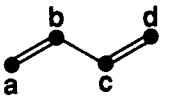

1

The two lowest energy Hückel molecular orbitals are ϕ_0 and ϕ_1.

$$\phi_0 \equiv \phi_{0a}a + \phi_{0b}b + \phi_{0c}c + \phi_{0d}d = 0.372(a + d) + 0.602(b + c)$$

$$\phi_1 \equiv \phi_{1a}a + \phi_{1b}b + \phi_{1c}c + \phi_{1d}d = 0.602(a - d) + 0.372(b - c) \quad (1)$$

The Hückel ground state, $\Psi_{H\bar{u}}$, is therefore eq 2,

$$\Psi_{H\bar{u}} = |\phi_0^+\phi_1^+\phi_0^-\phi_1^-| \quad (2)$$

where $\phi_i^{\pm}$ are the up-spin and down-spin forms of ϕ_i and where the outside bars of $|\phi_0^+\phi_1^+\phi_0^-\phi_1^-|$ represent the formation of a Slater determinant.

We now consider that portion of $\Psi_{H\bar{u}}$ where there are an equal number of electrons at each site. For instance, we calculate the portion of $\Psi_{H\bar{u}}$ where there are up-spin electrons on a and b and down spin electrons on c and d. We call this configuration $|a_+b_+c_-d_-|$.

$$\langle|a_+b_+c_-d_-|\psi_{H\bar{u}}\rangle = \begin{vmatrix}\phi_{0a} & \phi_{1a}\\ \phi_{0b} & \phi_{1b}\end{vmatrix}\cdot\begin{vmatrix}\phi_{0c} & \phi_{1c}\\ \phi_{0d} & \phi_{1d}\end{vmatrix} = 0.05 \quad (3)$$

In a similar manner we may calculate the components of $\Psi_{H\bar{u}}$ for all other configurations where there is one electron at each site. There are five other such configurations, i.e., $|a_-b_-c_+d_+|$, $|a_+b_-c_+d_-|$, $|a_-b_+c_-d_+|$, $|a_-b_+c_+d_-|$, and $|a_+b_-c_-d_+|$.

In other words, we are projecting $\Psi_{H\bar{u}}$ onto a space where there are a fixed number of electrons at each site. We call this projection operation P.

$$P\Psi_{H\bar{u}} = 0.05\{|a_+b_+c_-d_-| + |a_-b_-c_+d_+|\} - 0.25\{|a_+b_-c_+d_-| + |a_-b_+c_-d_+|\} + 0.20\{|a_-b_+c_+d_-| + |a_+b_-c_-d_+|\} \quad (4)$$

The crux of our method is the comparison of $P\Psi_{H\bar{u}}$ and Ψ_{He} where Ψ_{He} is the ground of the AF Heisenberg Hamiltonian of eq 5.

$$H_{He} = -\sum J_{ij}S_i\cdot S_j$$

$$\text{where } J_{ij} = \begin{cases} J \text{ for i and j that are bonded atoms,} \\ 0 \text{ otherwise} \end{cases} \quad (5)$$

Such Hamiltonians have proven to be useful for solid-state and inorganic clusters of magnetic materials[11] as well as for unsaturated hydrocarbons.[4,6,12] In the case of the π orbitals of butadiene the spin operators are for the spin-$^1/_2$ electrons and Ψ_{He} is given in eq 6. We have used a normalization constant in (6) which

$$\Psi_{He} = 0.07\{|a_+b_+c_-d_-| + |a_-b_-c_+d_+|\} - 0.25\{|a_+b_-c_+d_-| + |a_-b_+c_-d_+|\} + 0.18\{|a_-b_+c_+d_-| + |a_+b_-c_-d_+|\} \quad (6)$$

allows direct comparison to the $P\Psi_{H\bar{u}}$ of eq 4. It may be seen that Ψ_{He} and $P\Psi_{H\bar{u}}$ are rather similar. Our special interest here is in calculating spin–spin correlation terms, i.e., the degree to which the spin direction at atom i is correlated to the spin direction at atom j. We call the spin–spin correlation for these two atoms $C'(i,j)$.

$$C' \equiv \frac{4\langle\Psi_{He}|S_{iz}S_{jz}|\Psi_{He}\rangle}{\langle\Psi_{He}|\Psi_{He}\rangle} \quad (7)$$

In the projection operator Hückel (POH) method we approximate $C'(i,j)$ by eq 8. We compare $C'(i,j)$ to $C(i,j)$ for **1** in Figure 1.

$$C(i,j) \equiv \frac{4\langle\Psi_{H\bar{u}}|PS_{iz}S_{jz}P|\Psi_{H\bar{u}}\rangle}{\langle\Psi_{H\bar{u}}|\Psi_{H\bar{u}}\rangle} \quad (8)$$

It may be seen that the approximation is a good one.[7] The work described in ref 4–7 has shown that the method works well for systems with half-filled valence bands that are of alternant type geometry (i.e., contain only even-membered rings). It works especially well in the absence of rings.

The advantages of POH are 2-fold. The first is numerical. In Table I we compare the dimensions of the Hückel to the Heisenberg Hamiltonian. It may be seen that unless additional symmetries exist it becomes quite difficult to calculate Heisenberg Hamiltonians with more than 24 spin-sites.[13] The POH allows one to calculate up to (on a VAX 2000 workstation) 28 spin sites.

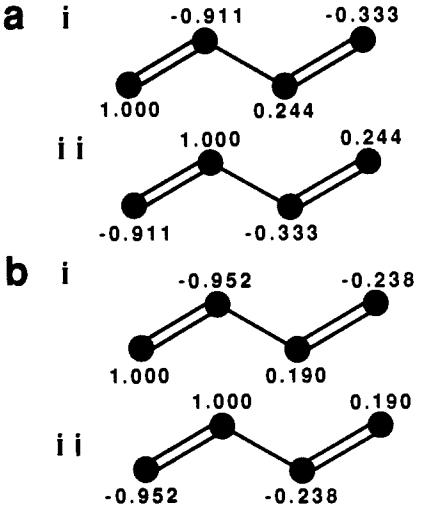

Figure 1. Spin–spin correlations for butadiene. (a) We show the $C(i,j)$ calculated by the POH method. We have assumed all β-interactions are of equal magnitude. In (i) we list $C(a,j)$ while in (ii) we list $C(b,j)$, see **1**. (b) The equivalent $C(i,j)$ calculated from the spin Hamiltonian. Note that both methods place a strong spin–spin correlation across the double bonds. This is especially clear in (aii) and (bii).

Table I. Comparison of the Size of $H_{H\ddot{u}ckel}$ and $H_{Heisenberg}$

no. atoms	dimension of $H_{H\bar{u}}$	dimension of H_{He}: Sz = 0 manifold	dimension of H_{He}: singlet manifold
4	4	6	2
10	10	252	42
18	18	48620	4862
26	26	10400600	742900

(10) (a) Bray, J. W.; Hart, H. R.; Interrante, L. V.; Jacobs, I. S.; Kasper, J. S.; Watkins, G. D. Wee, S. H.; Bonner, J. C. *Phys. Rev. Lett.* **1975**, *35*, 744. (b) Bray, J. W.; Interrante, L. V.; Jacobs, I. S.; Bonner, J. C. In *Extended Linear Chain Compounds*; Miller, J. S., Ed.; Plenum Press: New York, 1983; Vol. 3, p 353. (c) Whangbo, M.-H. *Inorg. Chem.* **1980**, *19*, 1728. (d) Whangbo, M.-H. *J. Chem. Phys.* **1981**, *75*, 4983.

(11) (a) See: Carlin, R. L. *Magnetochemistry*; Springer-Verlag: Berlin, 1986. (b) Pei, Y.; Verdauger, M.; Kahn, O. *J. Am. Chem. Soc.* **1986**, *108*, 7428. (c) Charlot, M.-F.; Kahn, O.; Chaillet, M.; Larrieu, C. *Ibid.* **1986**, *108*, 2574.

(12) (a) Ovchinnikov, A. A. *Theor. Chim. Acta* **1978**, *47*, 297. (b) Ovchinnikov, A. A. *Russ. Chem. Rev.* (*Engl. Transl.*) **1977**, *46*, 967. (c) Borden, W. T.; Davidson, E. R. *J. Am. Chem. Soc.* **1977**, *99*, 4587. (d) Berson, J. A.; Seeger, D. E. *J. Am. Chem. Soc.* **1983**, *105*, 5144. (e) Zilm, K. W.; Merrill, R. A.; Greenberg, M. M.; Berson, J. A. *J. Am. Chem. Soc.* **1987**, *109*, 1567. (f) Stone, K. J.; Greenberg, M. M.; Goodman, J. L.; Peters, K. S.; Berson, J. A. *J. Am. Chem. Soc.* **1986**, *108*, 8088. (g) Sugawara, T.; Bandow, S.; Kimura, K.; Iwamura, H. *J. Am. Chem. Soc.* **1984**, *106*, 6449. (h) Teki, Y.; Takui, T.; Itoh, K.; Iwamura, H. *J. Am. Chem. Soc.* **1983**, *105*, 3722.

(13) (a) Oitmaa, J.; Betts, D. D. *Can. J. Phys.* **1978**, *56*, 897. (b) Alexander, S. A.; Schmalz, T. G. *J. Am. Chem. Soc.* **1987**, *109*, 6933. (c) In the POH method, the controlling factor is that one actually generates an approximate Ψ_{He}. It will therefore never be the best numerical method for finding properties of Ψ_{He}.

Only quantum Monte Carlo methods allow larger systems (up to 100 spin-sites).[5] The second advantage is in the case where not all bonding interactions are equivalent. It is quite difficult in general to calculate the J_{ij}'s of eq 5. The Hückel or extended Hückel Hamiltonian is very easy to calculate with use of the Wolfsberg–Helmholtz[14] approximation. There are limitations to the method. The POH method does not include every type of magnetic interaction. For example, the 90° cation–anion–cation ferromagnetic effect has not been incorporated.[15] Therefore, the POH method is useful on systems where the Hückel β and the on-site repulsion U parameter (of the Hubbard model) are the dominant sources of the magnetic ordering. Generally though, the POH correlation effects when they do exist lead to very strong antiferromagnetic coupling. They are furthermore the only source for strong antiferromagnetic coupling. We therefore limit our study of AF ordering to systems with high Néel temperature, or in the case of one- or two-dimensional systems, systems with exchange constants near or exceeding room temperature.

n-Rings

Rings of n-spin-$^1/_2$ sites, such as the 10-ring compound **2** provide an introduction to the utility of the POH method. It may be viewed as a model representation of the 10π electrons in the cyclic

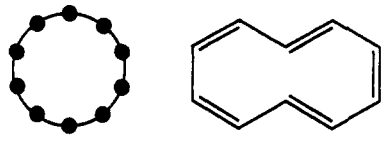

2a **2b**

unsaturated hydrocarbon $C_{10}H_{10}$. In Figure 2, we compare $C'(i,j)$ for the Heisenberg Hamiltonian to $C(i,j)$ based on the POH method. Such comparisons have previously been reported.[5,7] It may be seen that the POH method accurately predicts the true spin–spin correlation. In Figure 2b we show $C(i,j)$ for the 26-ring. It is difficult to directly compare our result here to the actual spin Hamiltonian $C'(i,j)$ as the spin Hamiltonian involves diagonalizing a 1×10^6 dimensional Hamiltonian. It is interesting to note that our results resemble Hirsch et al.'s[5] results on the Hubbard model using a quantum Monte Carlo simulation method.

$KCuF_3$

The $KCuF_3$ system is a tetragonally distorted perovskite.[8a,b] The distortion is due to the Jahn–Teller instability of octahedral Cu d^9 which reduces the Cu site symmetry from O_h to D_{2h}. We illustrate this structure in Figure 3. The magnetic structure of $KCuF_3$ is well characterized by single-crystal neutron diffraction and magnetic susceptibility measurements.[16] $KCuF_3$ is composed of linear strands of Cu that have a strong AF intrachain isotropic exchange constant of $J = -190$ K. These strands are shown in Figure 3. Between these chains there are much weaker ferromagnetic couplings and the system orders antiferromagnetically at 38 K. This magnetic structure is well understood theoretically by use of the Goodenough–Kanamori rules.[15] We show here that the antiferromagnetic exchange constants may also be understood via the POH method. We note the two methods use very different viewpoints: the former technique relies on valence bond ideas and super-exchange, while the latter one uses MO ideas.

In Figure 4 we show the MO diagram at Γ ($k = (0,0,0)$) where we have chosen as our unit cell a pseudo-cubic Cu_8F_{24} fragment. We have treated the potassium atoms in a Zintl fashion as mere electron donors. The Fermi level lies in the middle of the highest lying Cu d-orbital band. This d band has been split into two by the Jahn–Teller distortion. In Figure 3 we represent these orbitals

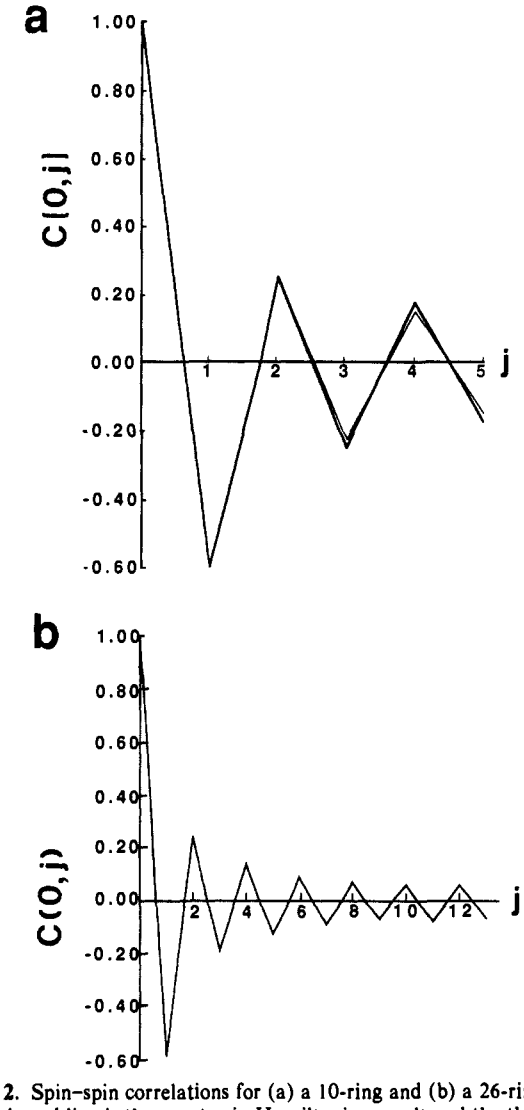

Figure 2. Spin–spin correlations for (a) a 10-ring and (b) a 26-ring. In (a) the broad line is the exact spin Hamiltonian result and the thin line is from a POH calculation. For both (a) and (b), j refers to the atom which is a jth nearest neighbor to the "zero"-atom, i.e., first nearest neighbor spin–spin correlation is $C(0,1)$ and $C(0,1) \approx -0.60$.

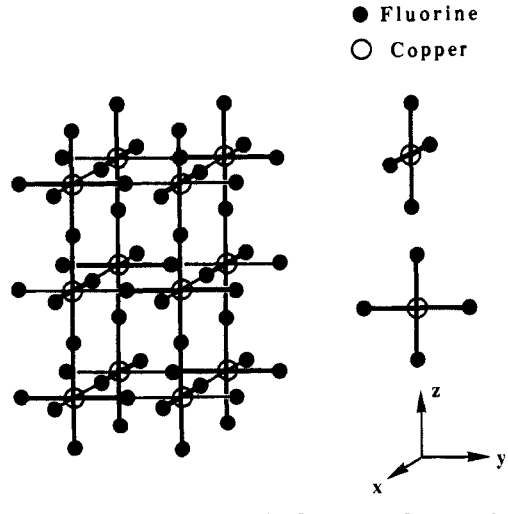

Figure 3. The tetragonal structure of $KCuF_3$. The Cu atoms have four shorter bonds of 1.89 and 1.96 Å and two longer 2.25-Å bonds. The four shorter bonds are all shown with an equivalent broad line and the longer ones by thin solid lines. Note that the Cu atoms are approximately square planar and that the square planes are oriented in two different ways.

as either $x^2 - y^2$ or $x^2 - z^2$ orbitals. These forms would be exactly correct were the distortion to have made a D_{4h} site symmetry at

(14) Wolfsberg, M.; Helmholz, L. *J. Chem. Phys.* **1952**, *20*, 837.
(15) (a) Goodenough, J. B. *Magnetism and the Chemical Bond*; J. Wiley: New York, 1963. (b) Kanamori, J. *J. Appl. Phys.* **1960**, *31*, 14S. (c) Kanamori, J. *Prog. Theor. Phys.* **1963**, *30*, 275.
(16) (a) Hirakawa, K.; Hirakawa, K.; Hashimoto, T. *J. Phys. Soc. Jpn.* **1960**, *15*, 2063. (b) Okazaki, A.; Suemune, Y. *J. Phys. Soc. Jpn.* **1961**, *16*, 671. (c) Hutchings, M. T.; Samuelsen, E. J.; Shirane, G.; Hirakawa, K. *Phys. Rev.* **1969**, *188*, 919. (d) Ikeda, H.; Hirakawa, K. *J. Phys. Soc. Jpn.* **1973**, *35*, 722. (e) Hirakawa, K.; Kurogi, Y. *Prog. Theor. Phys. Suppl.* **1970**, *46*, 147.

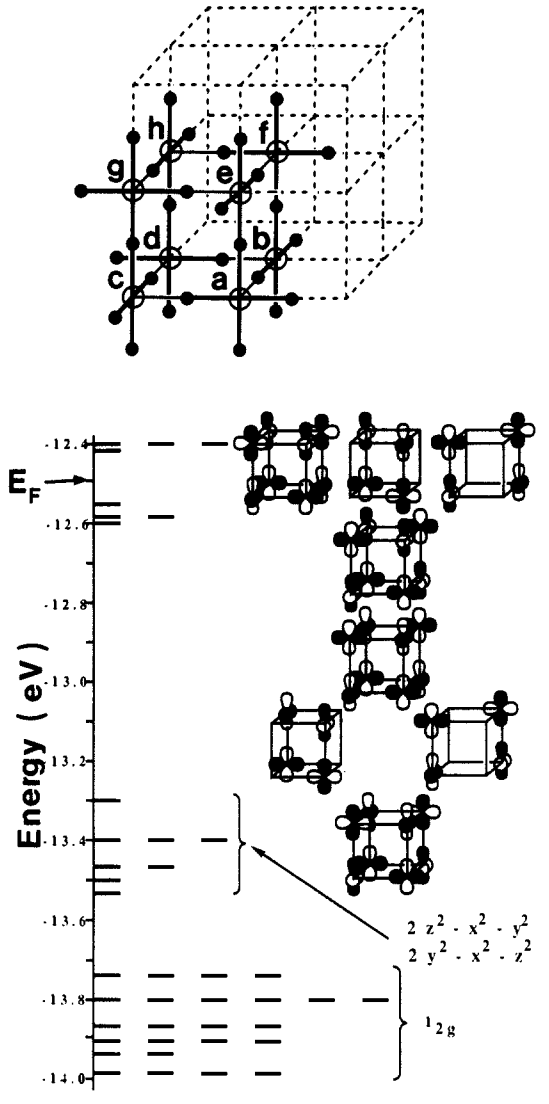

Figure 4. Molecular orbital diagram at Γ for an eight Cu atom unit cell of $KCuF_3$. At the top, the unit cell used is shown as the large cube. The eight inequivalent Cu atoms are also shown there. The calculation was done at Γ so all unit cells are in phase with each other. We show the MO levels of all the d-orbitals. We show the d-portion of the MOs for the eight highest energy d-orbitals. The bottom four are the filled orbitals while the top four are the unfilled ones. Note that for the four filled orbitals, the vertical lobes of the d-orbitals are all in phase. This is what is responsible for the experimentally found AF ordering. Extended Hückel parameters used are for Cu 4s (H_{ii} = −11.4 eV, ζ = 2.2), Cu 4p (H_{ii} = −6.06 eV, ζ = 2.2), Cu 3d (H_{ii} = −14.0 eV, ζ_1 = 5.95 (0.5933), ζ_2 = 2.30 (0.5749)), F 2s (H_{ii} = −40.0 eV, ζ = 2.425), and F 2p (H_{ii} = −18.1, ζ = 2.425). The K atoms were treated by using the Zintl concept as mere one-electron donors. No K-orbitals were used.

the copper atom positions. As the distortion leads to a D_{2h} site symmetry, the orbitals are more correctly $0.677x^2 - 0.734y^2 + 0.057z^2$ and $0.677x^2 - 0.734z^2 + 0.057y^2$ (the largest deviation from these values being $0.590x^2 - 0.784y^2 + 0.194z^2$). The actual form of the orbital, though, is not the most essential feature to our analysis. Rather, it is that to a good approximation (see values above) the eight MO's that span E_F are all linear combinations of the same eight atomic orbitals. We can therefore view this system as a one orbital per atom and a one electron per atom system. We may therefore reduce the extended Hückel calculation to a one orbital per atom model by means of an effective Hamiltonian approach. We have described this technique elsewhere.[61] The effective Hamiltonian approach results in eight molecular orbitals whose energies exactly mimic the energies of the eight orbitals that span the Fermi level in Figure 4. The matrix for this system uses as a basis set the effective localized atomic orbitals, denoted a–h in Figure 4. We now calculate $C(i,j)$ for these eight atomic orbitals. We show $C(a,j)$ in Figure 5. It may be seen

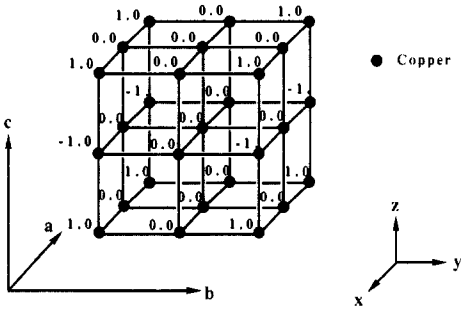

Figure 5. $C(i,j)$ for the eight Cu atom pseudo-cubic $KCuF_3$ cell. For $C(i,j)$ i is the corner atom of the cell shown. Hence at the corner of the large cube all $C(i,j)$ values equal 1 due to translational symmetry. Spin–spin correlation occurs only in the z direction. The orientation of the cube is the same as that in Figure 4.

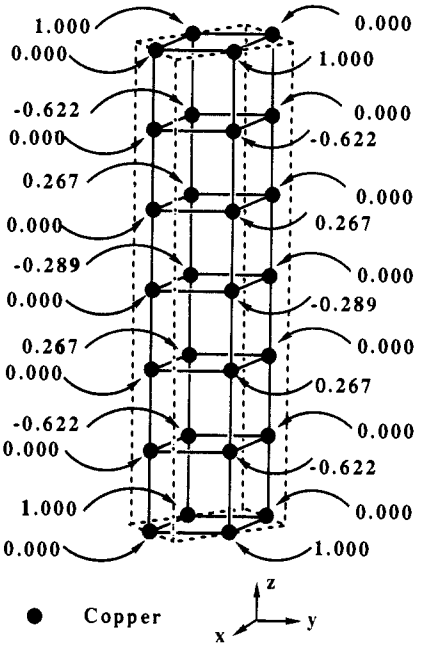

Figure 6. $C(i,j)$ for a twelve-atom $KCuF_3$ cell. The unit cell is indicated by the dotted lines. The orientation of the square-planar CuF_4 fragments is the same as in Figures 3 and 4. The parameters used are given in the caption of Figure 4.

that atom a is strongly correlated to one of the other seven atoms. Indeed, this is the direction of the strong antiferromagnetic coupling in $KCuF_3$. We show a similar calculation on a larger $Cu_{12}F_{36}$ cell in Figure 6. The local antiferromagnetic ordering is clear. It is also clear that the POH method does not lead to a prediction of the weak ferromagnetic coupling between chains. This is a natural limitation of the method. We have not included the effect of two electron exchange integrals that are known to be responsible for this effect.[15]

La_2CuO_4

Stoichiometric La_2CuO_4 is an antiferromagnet at low temperature.[17] It has a Néel temperature of 240 ± 10 K. This well-known structure contains sheets of vertex sharing octahedra.[9] In the center of these octahedra are copper atoms. These sheets are illustrated in Figure 7. This sheet structure undergoes a phase transition at 533 K. Above this temperature the phase is tetragonal and the sheets are planar while below this temperature the

(17) (a) Vaknin, D.; Sinha, S. K.; Moncton, D. E.; Johnston, D. C.; Newsam, J. M.; Safinya, C. R.; King, H. E., Jr., *Phys. Rev. Lett.* **1987**, *58*, 2802. (b) Yang, B. X.; Mitsuda, S.; Shirane, G.; Yamaguchi, Y.; Yamauchi, H.; Syono, Y. *J. Phys. Soc. Jpn.* **1987**, *56*, 2283. (c) Evain, M.; Whangbo, M.-H.; Beno, M. A.; Geiser, V.; Williams, J. M. *J. Am. Chem. Soc.* **1987**, *109*, 7917. (d) See also the AF ordering in $YBa_2Cu_3O_{6+x}$ in: Tranquada, J. M.; Cox, D. E.; Kunnmann, W.; Moudden, H.; Shirane, G.; Suenaga, M.; Zolliker, P.; Vaknin, D.; Sinha, S. K.; Alvarez, M. S.; Jacobson, A. J.; Johnston, D. C. *Phys. Rev. Lett.* **1988**, *60*, 156.

Table II. Spin–Spin Correlation for the Square Lattice Sheet of Cu Atoms in La_2CuO_4

		10 Cu atom cell[a]					
neighbor	Cu–Cu distance, Å	tetragonal	orthorhombic	1st nearest neighbor interactions only	18 Cu atom cell	22 Cu atom cell	26 Cu atom cell
1st nearest neighbor	3.82	−0.36	−0.36	−0.36	−0.39	−0.36	−0.36
2nd nearest neighbor	5.40 Å	(+0.25)	(+0.25)	(+0.25)	+0.19	+0.20	+0.19
3rd nearest neighbor	7.64				+0.16	+0.16	+0.15

[a] For the 10 atom cell the 2nd nearest neighbors are also 3rd nearest neighbors. Therefore, the $C(i,j)$ values are inflated.

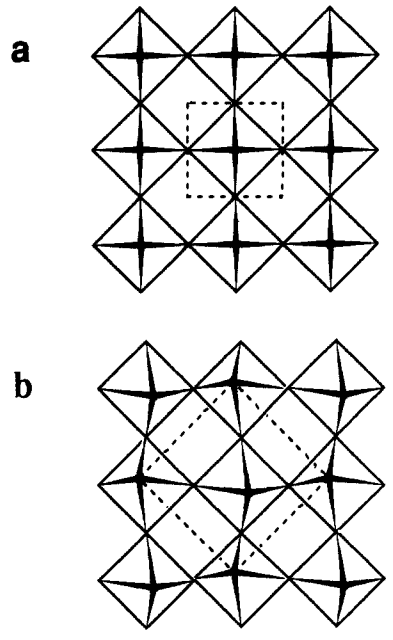

Figure 7. A single octahedral sheet of La_2CuO_4: (a) tetragonal form and (b) orthorhombic form. The copper atoms are at the center of the octahedra.

structure becomes orthorhombic and the sheets are buckled. As in $KCuF_3$, the copper have a d^9 electron configuration and these metal atoms therefore Jahn–Teller distort so as to have four short Cu–O bonds of 1.91 Å and two longer 2.46 Å bonds in La_2CuO_4. The long Cu–O bonds are parallel to one another, and therefore all the highest lying d-orbitals are oriented in the same fashion.

As Figure 7 shows, the connectivity of the highest lying d-orbitals is identical with those of s orbitals lying in a two-dimensional square lattice. We consider the molecular orbital diagram for the $Cu_{10}O_{40}$ unit cell shown in Figure 8. By our POH method this leads to estimates for the spin–spin correlation that are given in Table II. We show in Table II the spin–spin correlation values between atoms and their first, second, and third nearest neighbors. We have also performed this calculation on Γ for the unit cells shown in Figure 9. Of particular interest in Table II is the lack of any effect in $C(i,j)$ due to second nearest neighbor interactions. The columns for the 10-atoms Cu cell of Figure 8 show that it makes no matter if non-nearest-neighbor interactions are kept. We have therefore carried out the other calculations of Table II keeping only nearest-neighbor interactions. Finally, we have considered the effect of the orthorhombic distortion. As Table II shows the effect of this distortion also does not change the $C(i,j)$ values.

The results in Table II clearly show that the spin alternation of the Cu sublattice present in La_2CuO_4 is that of **3**.

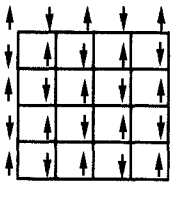

3

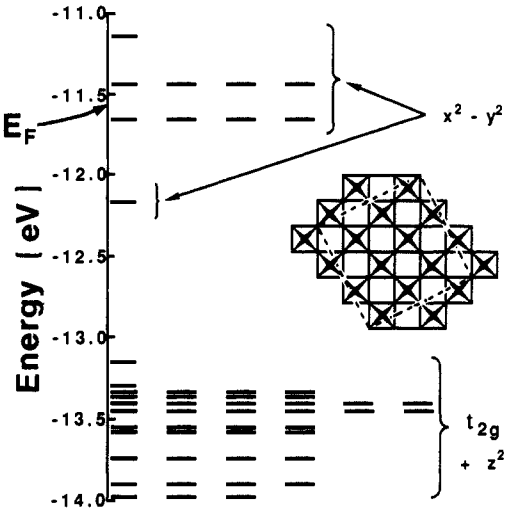

Figure 8. A molecular orbital diagram for a 10-Cu-atom cell. The extended Hückel parameters for the Cu atom are given in the caption of Figure 4. For O 2s H_{ii} = −32.3 eV and ζ = 2.275, and for O 2p H_{ii} = −14.8 eV and ζ = 2.275. The La atoms were considered to be mere three-electron donors and were not included in the calculation.

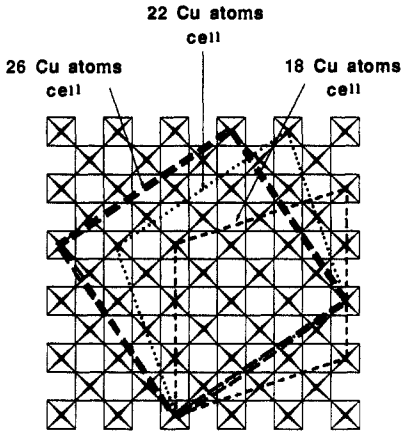

Figure 9. The 18-, 22-, and 26-Cu-atom cells.

Spin Peierls Distortions

Actual chemical systems that exhibit spin-Peierls distortions were first discovered 15 years ago.[10] The known examples are generally planar organometallic or organic molecules that stack on top of one another.[10] However, earlier theoretical work[18] had already suggested that under suitable conditions a Peierls-like distortion could occur in infinite chains, even if the undistorted state did not correspond to a metallic material but rather a nonconducting magnetic material. In this work they considered spin Hamiltonians such as

$$H(J,J') = -2\sum_i (JS_{2i}S_{2i+1} + J'S_{2i}S_{2i-1}) \qquad (9)$$

where J and J' are negative (i.e., AF) exchange parameters. These workers noted that if one considers the above Hamiltonian where

(18) (a) Duffy, W., Jr.; Barr, K. P. *Phys. Rev.* **1968**, *165*, 647. (b) Pincus, P. *Solid State Commun.* **1971**, *9*, 1971.

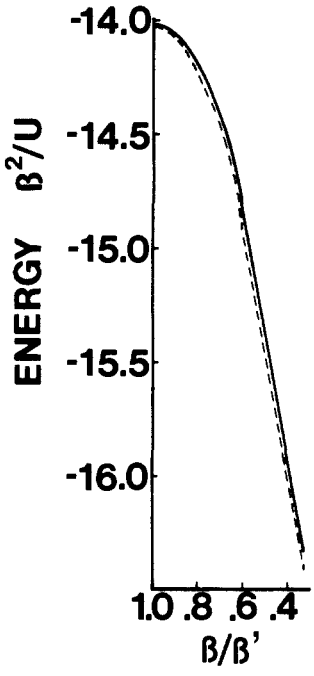

Figure 10. The AF Heisenberg and POH ground state energies for a 10-atom ring with bond strength alternation. The solid line is the POH approximation, and the dotted line is the true Heisenberg energy. The energy scale is set such that $E = 0$ corresponds to the ferromagnetic state.

J and J' are constrained such that $J + J'$ equals a constant then the ground state of $H(J,J')$ has a maximum at $J = J'$. This energy maximum provides the driving force for the distortion. This then is the original theoretical underpinning of the spin-Peierls distortion.

In this section we illustrate that the POH method can also be used to analyze the energies of the ground state of Hamiltonians such as that given in eq 9. In our comparison of $\Psi_{H\emptyset}$ vs Ψ_{He} we consider the Hückel Hamiltonian

$$H(\beta,\beta') = -\sum_i \beta|\phi_{2i}\rangle\langle\phi_{2i+1}| + \beta'|\phi_{2i}\rangle\langle\phi_{2i-1}| + \text{herm. conj.} \tag{10}$$

It is a well-known result of the Hubbard model that in the limit of electron localization (the regime where spin Hamiltonians are truly valid) J and J' are proportional to respectively β^2 and β'^2. We can therefore establish a Heisenberg Hamiltonian like that given in eq 9 which corresponds to the Hückel Hamiltonian of eq 10.

In Figure 9 we compare E_{He} and E_{POH} where

$$E_{He} = \langle\Psi_{He}|H(J,J')|\Psi_{He}\rangle \tag{11}$$

$$E_{POH} = \langle\Psi_{H\emptyset}|PH(J,J')P|\Psi_{H\emptyset}\rangle \tag{12}$$

We consider a ring of ten atoms (as $H(J,J')$ otherwise grows to a larger than 10^3 dimensional matrix). We have used as a constraint in our calculations that $\beta + \beta'$ is kept constant. In Figure 10 we compare the energy of $P\Psi_{H\emptyset}$ to that of the Heisenberg Hamiltonian as we vary the β in the Hückel Hamiltonian. It may be seen that the POH method provides a good approximation to the true ground-state energy. Due to the variational principle, it provides an upper bound.

Nonalternant Systems

In the previous examples we have restricted our attention to alternant systems,[19] i.e., systems that do not contain odd-member rings. We mentioned earlier that the reason for this is that there exist odd-member-ring systems for which the correspondence between the projected operator Hückel and Heisenberg ground states is poor. Recently, some workers have shown that charge transfer is an important problem in these systems.[6]

We therefore, at first, will restrict our attention to a model nonalternant system in which charge transfer is minimized. We consider the system **4** for which every site is equivalent (hence no net charge transfer can occur although greater charge fluctuation is possible[20]). A chemical example of this is the W atoms in WTe_2. We consider that each vertex in **4** is the site of a single

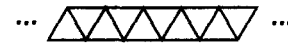

4

half-filled orbital. There is therefore one electron at each site. As the system is an extended solid we consider a unit cell of varying size. This is equivalent to the fragment within the solid approach.[21] Thus, **5** and **6** are both approximations to **4** representing respectively eight- and ten-atom cells. Their respective symmetries

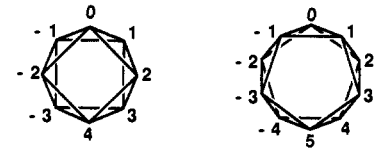

5 **6**

are D_{4d} and D_{5d}. In Table III we show the $C(i,j)$'s for these systems. The agreement between the POH and Heisenberg values is poor. For **5**, a comparison of Ψ_{He} and $P\Psi_{H\emptyset}$ shows that $\langle\Psi_{He}(5)|P|\Psi_{H\emptyset}(5)\rangle = 0$. The former wave function is of $^1B_1$ symmetry, while the latter is of $^1A_1$ symmetry. We have called this change in ground state in an earlier paper a Hubbard transition.[6] It is the molecular analogue of the Mott transition.[24]

It is an interesting question as to whether **4** also undergoes a Hubbard transition. We have therefore compared Ψ_{He} and $\Psi_{H\emptyset}$ for the two low-symmetry systems **7** and **8**.

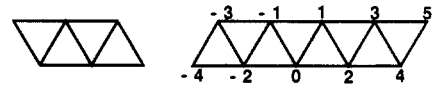

7 **8**

Using normalized $P\Psi_{H\emptyset}$ and Ψ_{He} we find

$$\langle\Psi_{He}(7)|P|\Psi_{H\emptyset}(7)\rangle = 0.852 \tag{13}$$

$$\langle\Psi_{He}(8)|P|\Psi_{H\emptyset}(8)\rangle = 0.287 \tag{14}$$

Table III. Comparison of POH and Heisenberg Spin-Spin Correlation Functions for Fragments of System **4**

j	$C(0,j)$ for **5** from POH	$C'(0,j)$ for **5** from Heisenberg	$C(0,j)$ for **8** from POH	$C'(0,j)$ for **8** from Heisenberg	$C'(0,j)$[a] for **6** from Heisenberg
−4			0.063	0.139	0.067
−3	−0.154	0.037	−0.074	−0.036	0.213
−2	−0.308	−0.628	−0.561	−0.478	−0.461
−1	−0.154	−0.061	−0.055	−0.159	−0.207
0	1.000	1.000	1.000	1.000	1.000
1	−0.154	−0.061	−0.037	−0.570	−0.207
2	−0.308	−0.628	−0.369	−0.413	−0.461
3	−0.154	0.037	−0.016	−0.284	0.213
4	0.231	0.302	0.047	0.155	0.067
5			0.001	−0.240	−0.224

[a] The POH values for **6** are not listed as there is a degeneracy in the Hückel Fermi level for this system.

(19) Coulson, C. A.; Rushbrooke, G. S. *Proc. Cambridge Philos. Soc.* **1940**, *36*, 193.

(20) (a) Anderson, P. W. *Mater. Res. Bull.* **1973**, *8*, 153. (b) Hirakawa, K.; Kadowaki, H.; Ubukoshi, K. *J. Phys. Soc. Jpn.* **1985**, *54*, 3526. (c) Jullien, R.; Penson, K. A.; Pfeuty, P.; Uzelac, K. *Phys. Rev. Lett.* **1980**, *44*, 1551.

(21) See: Burdett, J. K. *Molecular Shapes*; J. Wiley: New York, 1980; pp 271–275.

(22) Mott, N. F. *Proc. Phys. Soc. (London)* **1949**, *A62*, 416.

(23) (a) Hay, P. J.; Thibeault, J. C.; Hoffmann, R. *J. Am. Chem. Soc.* **1975**, *97*, 4884. (b) Estes, W. E.; Gravel, D. P.; Hatfield, W. E.; Hodgson, D. J. *Inorg. Chem.* **1978**, *17*, 1415.

(24) Brec, R. *Solid State Ionics*, **1986**, *22*, 3 and references therein.

It therefore appears likely that as the open chain grows infinitely long, the dot product tends to zero, i.e.,

$$\langle \Psi_{He}(4)|P|\Psi_{H\bar{u}}(4)\rangle = 0 \qquad (15)$$

This is compatible but is certainly not sufficient to prove that **5** which is of "$D_{\infty d}$" symmetry may possess a Hubbard transition.

Finally, we contrast our above results with our result on *n*-rings. For **2** we find

$$\langle \Psi_{He}(2)|P|\Psi_{H\bar{u}}(2)\rangle = 0.998 \qquad (16)$$

If we recall that **2** and **8** are both ten-atom systems, we see the profound effect nonalternacy may have. For instance, one would suppose that systems like the single-strand one-dimensional chain and **4** would have very different metal-insulator transitions even though both are one-dimensional systems. This shows that the topology of the system is just as important if not more important that the dimneisonality.

Conclusion

Fifteen years ago Hay, Thibeault, and Hoffmann[23] published a study on the exchange constants found in Cu^{II} dimers such as **9** and **10**, where L was a ligand such as a halide, hydroxide, or

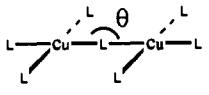

9

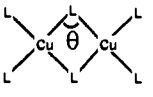

10

alkoxide and θ was a variable angle. Using a simple extended Hückel method they were able to establish a relationship between θ and the sign of the exchange constant. J_{Cu-Cu} is antiferromagnetic at $\theta = 180°$ while J_{Cu-Cu} is ferromagnetic at $\theta = 90°$. In the 90° case they showed that there was no driving force for the formation of a singlet ground state and they therefore assumed that the electrons would follow Hund's rule and align in a parallel fashion. In this article we have shown that this same approach is also valid in solid-state systems. In the POH method, AF ordering is revealed by strongly correlated spin orientations. In the absence of such strong correlations we might assume ferromagnetic exchange (derived from direct exchange between localized orbitals with ligand contributions) can dominate. This is what happens in $KCuF_3$. As in the earlier work[24] on molecular systems the POH method has the defect of not predicting the absolute size of these AF exchange constants. This drawback is due to the exchange constants being approximately[5-7]

$$J = -2\beta^2/U \qquad (17)$$

where β is the Hückel interatomic hopping integral and U is the on-site repulsion. While β may be evaluated by a Hückel calculation, U cannot be. We see though that relatively small β's (the band width of the highest lying d orbitals is 0.20 and 1.00 eV for respectively $KCuF_3$ and La_2CuO_4) can lead to reasonably large J values (near 200 K for $KCuF_3$). More studies need to be carried out before an understanding of absolute J values can be obtained.

In this article, we have given two examples of the interplay of spatial distortion and type of antiferromagnetic ordering. In the case of $KCuF_3$ the cubic to tetragonal distortion is responsible for the AF ordering of that system. However, the tetragonal to orthorhombic distortion in La_2CuO_4 plays no discernable role in the La_2CuO_4 AF ordering.

The final success of the POH method will certainly depend on the ability of the method to handle other more complicated systems. $MnPS_3$ and $FePS_3$ are ideal candidates for future study. These two systems are isostructural. Both contain a graphite sheet of transition-metal atoms, **11**. However, in the two cases the reported orderings are different. $MnPS_3$ has the ordering shown in **12** while $FePS_3$ has the ordering shown in **11**. As this example

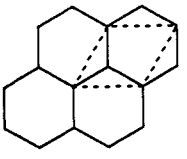

11

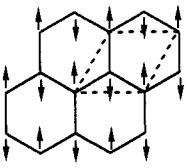

12

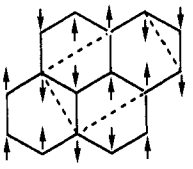

13

shows, even for alternant systems, the AF ordering is not always of one type. [One might imagine that **13** was the only logical AF ordering.] To study the systems the POH method will have to be successfully extended to more complex d-electron counts.

Acknowledgment. The extended Hückel programs used in this work were originally developed by R. Hoffmann and his coworkers. M.-H. Whangbo, M. Evain, T. Hughbanks, S. Wijeyesekera, M. Kertesz, C. N. Wilker, and C. Zheng have all contributed to its current form. I would like to thank J. Burdett and his group for providing me with a copy of this program and the donors of the Petroleum Research Fund, administered by the American Chemical Society, and the Rackham Graduate School for their financial support.